Fabrication of copper nanowires via electrodeposition in anodic aluminum oxide templates formed by combined hard anodizing and electrochemical barrier layer thinning

Stepniowski, Wojciech J.; Moneta, Marcin; Karczewski, Krzysztof; Michalska-Domanska, Marta; Czujko, Tomasz; Mol, Johannes M.C.; Buijnsters, Josephus G.

DOI
10.1016/j.jelechem.2017.12.052

Publication date
2018

Document Version
Final published version

Published in
Journal of Electroanalytical Chemistry

Journal of Electroanalytical Chemistry 809 (2018) 59–66

Contents lists available at ScienceDirect

Journal of Electroanalytical Chemistry

journal homepage: www.elsevier.com/locate/jelechem

Fabrication of copper nanowires via electrodeposition in anodic aluminum oxide templates formed by combined hard anodizing and electrochemical barrier layer thinning

Wojciech J. Stepniowski[a,b,c,*], Marcin Moneta[a], Krzysztof Karczewski[a], Marta Michalska-Domanska[d], Tomasz Czujko[a], Johannes M.C. Mol[b], Josephus G. Buijnsters[c]

[a] Department of Advanced Materials and Technologies, Faculty of Advanced Technology and Chemistry, Military University of Technology, Kaliskiego 2 Str., 00-908 Warszawa, Poland
[b] Delft University of Technology, Department of Materials Science and Engineering, Faculty 3mE, Mekelweg 2, 2628 CD Delft, The Netherlands
[c] Delft University of Technology, Department of Precision and Microsystems Engineering, Faculty 3mE, Mekelweg 2, 2628 CD Delft, The Netherlands
[d] Institute of Optoelectronics, Military University of Technology, Kaliskiego 2 Str., 00-908 Warszawa, Poland

ARTICLE INFO

Keywords:
Anodizing
Anodic aluminum oxide
Self-organization
Hard anodizing
Electrochemical barrier layer thinning
Electrodeposition
Copper nanowires

ABSTRACT

Anodic aluminum oxide was formed by employing mild and hard anodizing in sulfuric acid followed by mild anodizing in oxalic acid without oxide removal in-between at 40 and 45 V. Such multi-step anodizing, combining hard anodizing in sulfuric acid with mild anodizing in oxalic acid allowed to form a highly-ordered nanoporous template with a barrier layer at the pore bottoms thin enough for further processing. Four different conditions of electrochemical barrier layer thinning, with varied voltage steps and their time durations, were investigated. Optimized conditions allowed to provide conductivity at the pore bottoms and made the nanoporous oxide templates suitable for electrodeposition. It was found that the most effective barrier layer thinning approach employs voltage steps $U_{n+1} = 0.75 \cdot U_n$ with each step (n) being 10 s long. To check applicability of the formed templates, copper electrodeposition from sulfate-borate bath was done. Copper nanowires with average length of about 14–16 μm and diameter of about 35–40 nm were obtained by using through-hole AAO templates.

1. Introduction

Self-organized anodization of aluminum and its alloys is generally considered as a method for corrosion protection [1]. Furthermore, since 1995 when two-step self-organized anodization was first reported by Masuda and Fukuda [2], aluminum anodizing triggered much fundamental research on tuning of morphology by operating conditions and first approaches in template-assisted nanofabrication. The morphological features of nanoporous anodic aluminum oxide (AAO) like pore diameter, interpore distance, thickness of the grown oxide and further derivatives like barrier layer thickness or thickness of the oxide wall, can be controlled by anodizing conditions including type, concentration and temperature of the electrolyte, anodizing voltage, viscosity of the electrolyte, or duration of anodizing [3–4].

Currently, numerous new strategies are being researched, including anodizing in novel electrolytes [5–6], in viscous electrolytes [7], with additives [8–9], or by changing current or voltage during the anodizing process resulting in a formation of 3D patterns [10–11].

Nanoporous AAO has become one of the most commonly applied templates in nanofabrication due to its distinctive morphology control and cost efficiency of fabrication. For example, inexpensive aluminum substrates were successfully anodized, providing a well-ordered, nanoporous oxide [11]. With the use of various techniques, including: electrodeposition, chemical vapor deposition, spin coating, physical vapor deposition, sol-gel technique etc. nanowires, nanotubes and nanodots made of metals [12–13], semiconductors [14], superconductors [15], polymers [16] and carbon materials [17] were formed triggering advances on and optical materials and renewable energy harvesting [14], sensing, or highly adhesive materials [16].

To form nanostructures with the use of anodic aluminum oxide templates, a multi-step approach is required. After two step anodizing [2], removal of the remaining aluminum (i.e. with $HgCl_2$) and opening of the pore bottoms are required in order to remove the oxide barrier layer and obtain through-hole membranes. Furthermore, in case of metallic nanowires (NW) formation via electrodeposition, gold sputtering and short gold electrodeposition from a cyanide bath are

* Corresponding author at: Department of Advanced Materials and Technologies, Faculty of Advanced Technology and Chemistry, Military University of Technology, Kaliskiego 2 Str., 00-908 Warszawa, Poland.
E-mail addresses: wojciech.stepniowski@wat.edu.pl, W.J.Stepniowski-2@tudelft.nl (W.J. Stepniowski).

https://doi.org/10.1016/j.jelechem.2017.12.052
Received 24 October 2017; Received in revised form 18 December 2017; Accepted 20 December 2017
Available online 21 December 2017
1572-6657/

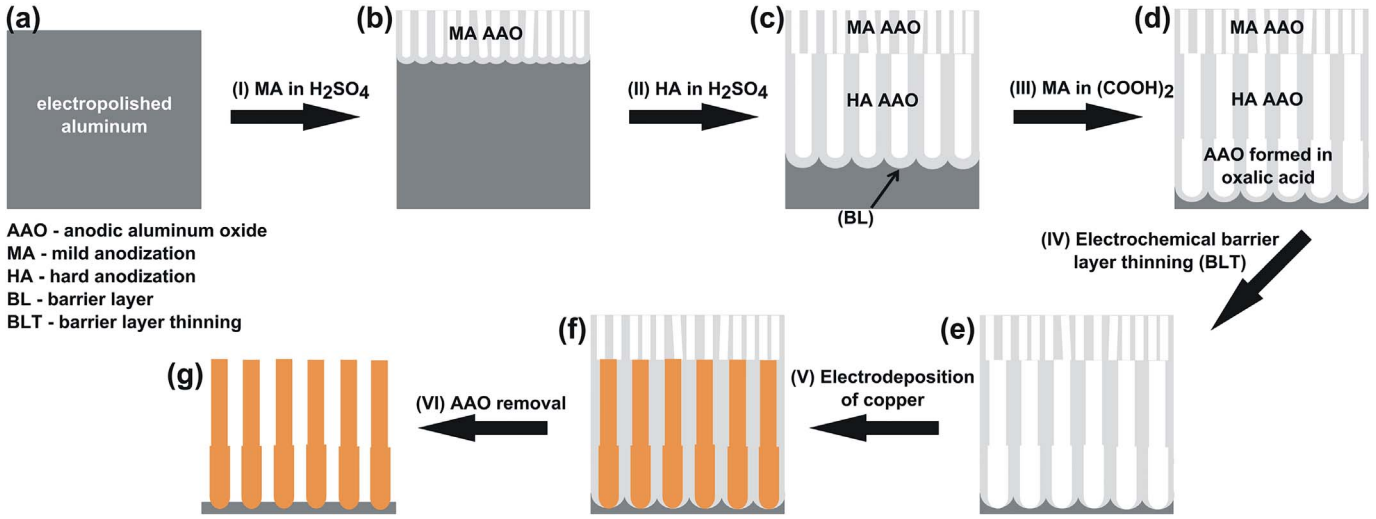

Fig. 1. Schematic representation of template-based fabrication of copper nanowires: (a) degreased and electropolished aluminum foil was subjected to mild anodization (MA) in sulfuric acid (I) and nanoporous protective oxide layer was formed (b); hard anodizing in sulfuric acid (II) allowed to obtain highly-ordered AAO (c); anodizing was continued in oxalic acid (III) and AAO with thinner oxide barrier layer was obtained (d); barrier layer thinning was performed (IV) and barrier layer was thus further thinned (e); electrodeposition of copper (V) allowed to form copper nanowires (f); anodic alumina was removed (VI) and free-standing Cu nanowires were obtained (g).

required to provide sufficient electrical contacts at the pore bottoms [13]. Thus, the multi-step approach is time consuming, despite the fact that the fabrication of anodic alumina templates itself is inexpensive. An elegant alternative was proposed by Furneaux et al. [18]. After anodizing, the pores at the bottom of AAO templates were opened by using a quasi-exponential voltage decrease, and, as a result, conductive (aluminum) substrate was exposed to the electrolyte. Therefore, this approach, in further studies, allowed for nanofabrication of metallic nanowires [19–20]. The electrochemical barrier layer thinning (BLT) was then developed by Choi et al. [19–20]. They succeeded in the formation of monodisperse silver nanowires by using anodic alumina templates with an electrochemically perforated barrier layer. With the use of this approach, nanowires and nanotubes made of Au [21], Bi [22] and Ni [12,23–25] have been synthesized successfully.

Arrangement and uniformity of the nanopores in AAO templates are also important for nanofabrication, because a narrow distribution of the diameter of nanowires and nanotubes is required in further applications, where size-induced phenomena occur. For this reason, hard anodizing (HA), an approach providing highly-ordered AAO, is also applied. The process is conducted at relatively high voltages (40–70 V for H_2SO_4), higher than maximal values applied in standard, mild anodizing (up to 25 V for H_2SO_4). To prevent the aluminum anode from destruction by the high density avalanche current, known as “burning”, firstly a protective oxide layer is grown at standard (mild) voltage and then the voltage is increased [26]. As a result, improved ordering of AAO is achieved. Chu et al. reported a convincing study, where ordering of AAO formed with mild anodizing at 25 V in sulfuric acid and hard anodizing at 40 and 70 V in sulfuric acid are compared [27]. It is clearly shown that hard anodizing provides much better ordering, which is in line with previous observations reported by Ono et al. [28], showing improved ordering of AAO formed in organic acids at high voltages. However, during high-field/hard anodizing, high current densities flow through the circuit and much Joule's heat is secreted. Thus, to minimize this effect various modifiers are added to the electrolyte, like ethylene glycol (EG) increasing viscosity of the electrolyte and decreasing ionic mobility, resulting in lower current densities at the same voltage and less heat at the anode [29].

The major motivation of the conducted research was to obtain highly-ordered AAO templates with barrier layers opened at the bottom, employing a facile and cost-effective approach. Successful electrodeposition of highly uniform copper nanowires with the aid of thus produced through-hole templates confirms the applicability of the proposed method.

2. Experimental

2.1. Preparation of the samples

Commercial purity aluminum alloy (AA 1050 alloy) was cut into coupons (40 mm × 20 mm × 0.5 mm), degreased (acetone, ethanol) and electropolished ($EtOH:HClO_4$ 4:1, 0 °C, 20 V, 120 s, Pt cathode grid). Next, the samples were covered with acid resistant lacquer at the back and edges and 4 cm^2 working area was exposed and used in further processing. All the electrochemical processes were performed in a double-walled electrochemical cell connected with a LAUDA A100/RA 100 thermostat in order to provide constant, controllable temperature. Processes were carried out using a DC power supply (NDN DF1730SL5A) and current densities were being recorded with an APPA 207 multimeter.

In order to obtain desired nanoporous AAO templates and perform further nanofabrication, a multistep procedure was employed (Fig. 1). Firstly, mild anodization (MA) in 0.5 M sulfuric acid with 20 vol% ethylene glycol (EG) was performed at 0 °C, 20 V, 60 min (Fig. 1, reaction I). Immediately after, the voltage was being increased with 0.5 V steps, each 5 s long, up to 45 V. Then, hard anodizing at 45 V was carried out for 1 h (Fig. 1, reaction II). Finally, in order to obtain AAO with thinner barrier layer at the bottom, 30 min of mild anodizing in 0.3 M $(COOH)_2$, at 45 V, 30 °C was performed (Fig. 1, reaction III).

Subsequently, after anodizing, electrochemical barrier layer thinning (BLT) was performed in 0.3 M $(COOH)_2$ (Fig. 1, reaction IV). To search for the optimum method, four different BLT process conditions were tested, i.e. the stepwise voltage decrease and the duration of each voltage step, according to:

1. $U_{n+1} = 0.5 \cdot U_n$; $\Delta t = 60$ s
2. $U_{n+1} = 0.75 \cdot U_n$; $\Delta t = 60$ s
3. $U_{n+1} = 0.5 \cdot U_n$; $\Delta t = 10$ s
4. $U_{n+1} = 0.75 \cdot U_n$; $\Delta t = 10$ s

To ensure that the pores were effectively opened at the bottom, aluminum was being chemically removed in a mixture of 0.1 M $CuCl_2$ in

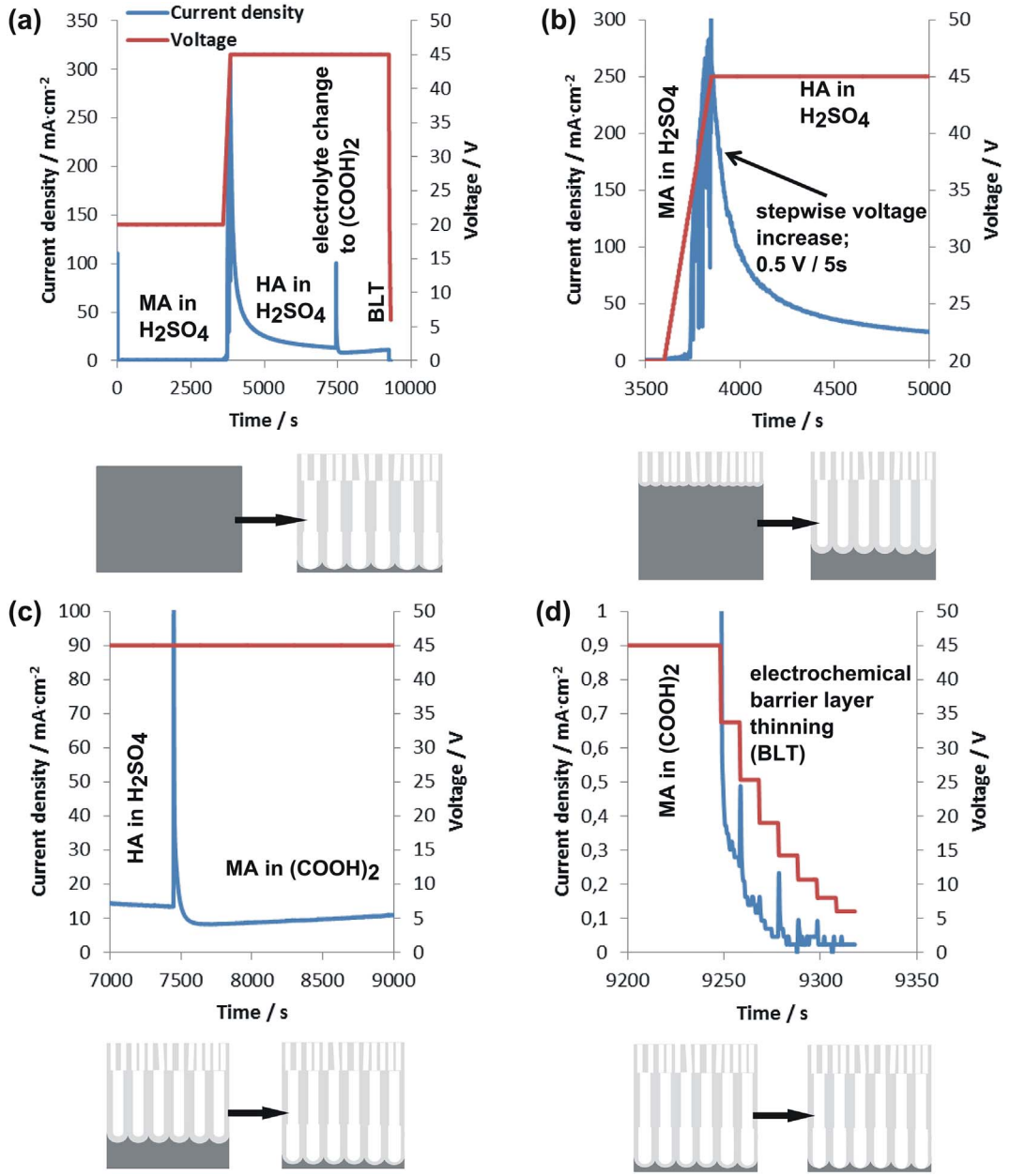

Fig. 2. Current density and voltage vs. time graphs: (a) complete current density and voltage vs. time, (b) mild to hard anodizing transition, (c) electrolyte change from sulfuric acid (hard anodizing regime) to oxalic acid (mild anodizing regime), (d) electrochemical barrier layer thinning (BLT) with voltage steps $U_{n+1} = 0.75 \cdot U_n$ (single step duration, Δt, is 10 s). The treatment effects on the formed AAO template are schematically depicted in the corresponding bottom pictures.

HCl and observed with field emission scanning electron microscopy (FE-SEM) from the bottom side.

Optimized BLT procedure was also applied for templates formed at 40 V, in order to confirm applicability of the method for AAO formed at different voltage.

To confirm the applicability of the membranes formed with combination of MA, HA and BLT, copper electrodeposition was performed. The electrodeposition was conducted directly through the oxide membranes with the use of an ATLAS 0531 (Atlas-Sollich, Poland) potentiostat with Pt counter electrodes and Ag|AgCl reference electrode. Electrodepositions were conducted at room temperature from 0.3 M $CuSO_4$ and 0.1 M H_3BO_3 solution at − 0.3 V vs. Ag|AgCl for 30 min (Fig. 1, reaction V). To liberate formed Cu nanowires (NW) from the AAO template, chemical etching in 5% H_3PO_4 was performed at 30 °C for 45 min (Fig. 1, reaction VI).

2.2. Sample characterization

Characterization of the samples' morphology (anodic alumina and copper nanowires) was done with a field emission scanning electron microscope (FE-SEM) Quanta 3D FEG (FEI, Phillips, The Netherlands). Image processing with NIS-Elements software (Nikon) was done in order to obtain quantitative data on the average diameter of the AAO pore bottoms and average diameter and length of the electrodeposited Cu nanowires, respectively. To obtain reliable data, at least 200 nanowires were analyzed to obtain average diameter and length.

The phase structure of the aluminum alloy surface after copper electrodeposition was analyzed by X-ray diffraction using a Rigaku Ultima IV diffractometer with Co K radiation (λ = 1.78897 Å) and operating parameters of 40 mA and 40 kV with a scanning speed of 1°/min and step size of 0.02°.

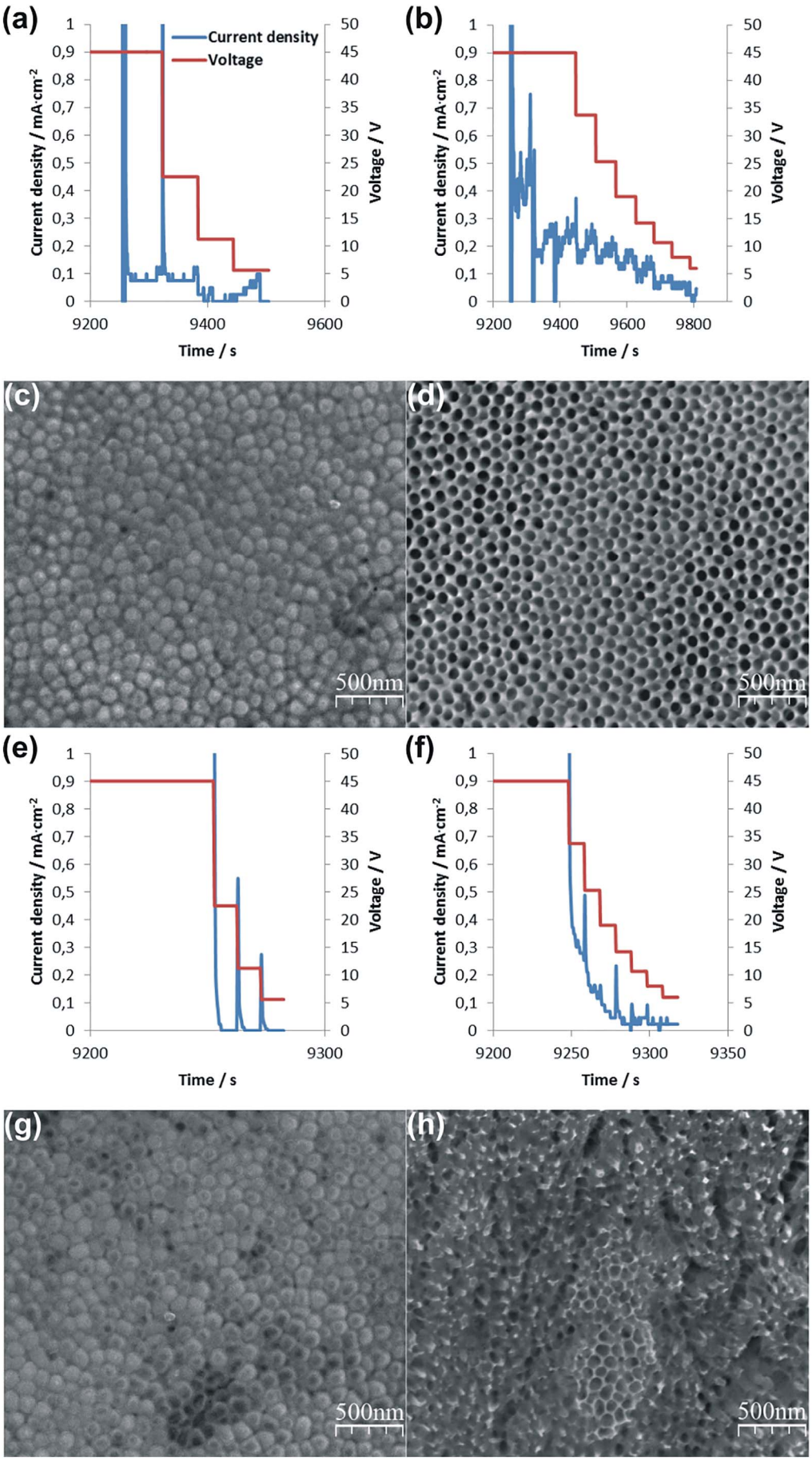

Fig. 3. Partial current density and voltage vs. time graphs for various electrochemical barrier layer thinning procedures (a, b, e, f) with FE-SEM micrographs of the AAO bottoms showing the BLT effects (c, d, g, h): (a, c) $U_{n+1} = 0.5 \cdot U_n$; $\Delta t = 60$ s, (b, d) $U_{n+1} = 0.75 \cdot U_n$; $\Delta t = 60$ s, (e, g) $U_{n+1} = 0.5 \cdot U_n$; $\Delta t = 10$ s, (f, h) $U_{n+1} = 0.75 \cdot U_n$; $\Delta t = 10$ s. The FE-SEM micrographs are bottom-view images after Al removal by 0.1 M $CuCl_2$ in HCl.

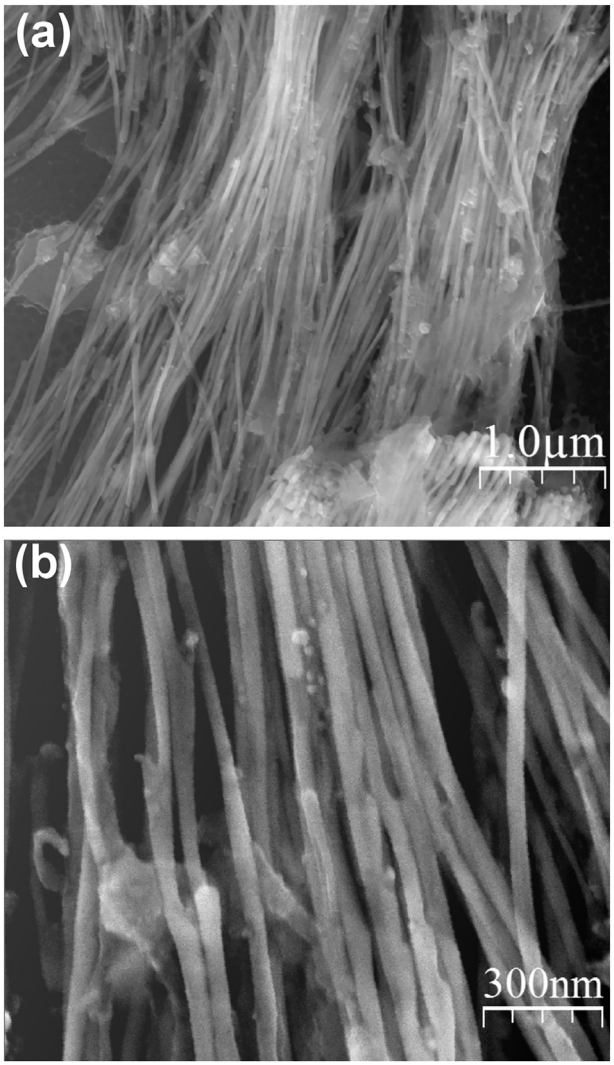

Fig. 4. Copper nanowires grown by electrodeposition into AAO templates formed with electrochemical barrier layer thinning employing $U_{n+1} = 0.75 \cdot U_n$; $\Delta t = 10$ s. Electrodeposition of copper was done in AAO formed at 45 V.

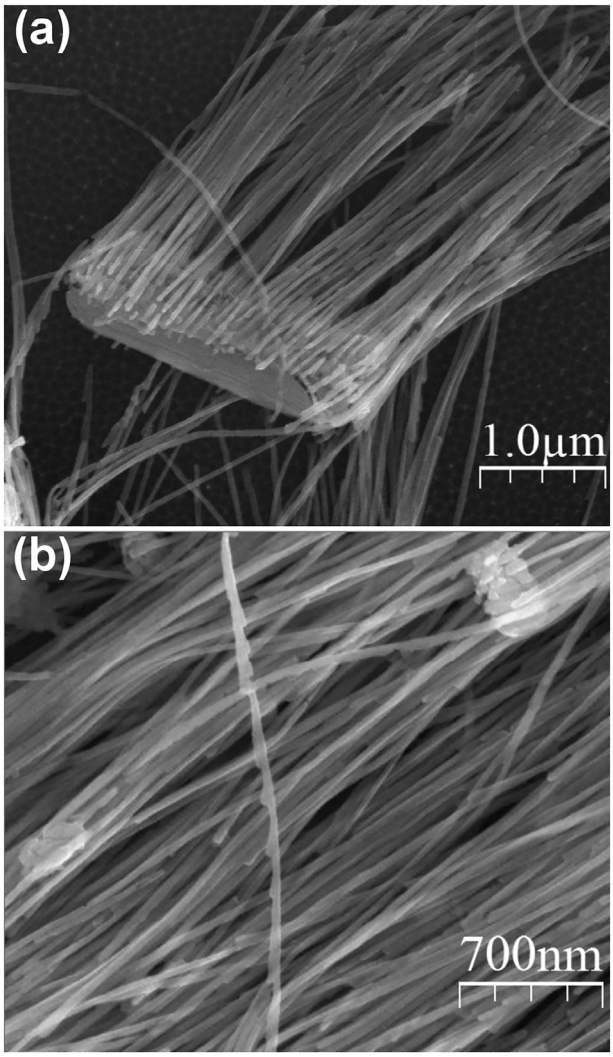

Fig. 5. Copper nanowires grown by electrodeposition into AAO templates formed with electrochemical barrier layer thinning employing $U_{n+1} = 0.75 \cdot U_n$; $\Delta t = 10$ s. Electrodeposition of copper was done in AAO formed at 40 V.

Table 1
Average diameter, length and aspect ratio of copper nanowires formed by direct electrodeposition into AAO formed at 40 and 45 V, respectively. Data were obtained by averaging of 5 FE-SEM images (corresponding to about 200 nanowires per voltage condition).

Voltage of AAO template formation/V	Diameter of nanowires/nm	Length of nanowires/μm	Aspect ratio
40	35 ± 6	14.4 ± 2.7	410
45	40 ± 5	15.7 ± 1.0	400

3. Results and discussion

Fig. 2 depicts the voltage and current vs. time evolution during the anodization process (upper row) together with the effects of the anodizing treatment on the formed AAO template (lower row). Firstly, typical mild anodizing (MA) in sulfuric acid was performed at 20 V for the first hour (Figs. 2a and 1, reaction I). To achieve a high level of ordering, hard anodizing (HA) at 45 V (Fig. 1, reaction II) was then performed, after a stepwise increase of the anodizing voltage was applied (Fig. 2b). In each step, the voltage was 0.5 V higher than in the previous step (each step 5 s long). Once 45 V was achieved (hard anodizing regime, providing much better ordering), the voltage was being kept constant for 1 h. Hard anodization of aluminum in sulfuric acid provided AAO with a thick barrier layer at the bottom. Thus, electrochemical barrier layer thinning would not be possible subsequently after HA in sulfuric acid (no current response was registered during BLT right after HA in sulfuric acid during preliminary experiments). Therefore, a process that allows to decrease the thickness of the barrier layer before electrochemical barrier layer thinning was added to the procedure. Anodization in oxalic acid allowed to form AAO with a much thinner barrier layer. Such electrolyte change also allowed to maintain the pore ordering resulting from the HA process (moreover, anodizing in oxalic acid at 45 V provides satisfactory ordering of the pores as well [30]). Anodization in oxalic acid at 45 V is a MA regime, thus the current density and resulting oxide growth rate are typically much smaller, which can also be observed from the experimental data in Fig. 2c (see also Fig. 1, reaction III). Due to the application of the same voltage, while changing the electrolyte from sulfuric acid to oxalic acid, the interpore distance and ordering inherited from HA were maintained. Nevertheless, pore diameter varied, resulting in a thinner barrier layer at the bottom, enabling the BLT process. During HA, AAO grows much faster and the secondary etching reaction between the grown oxide and acidic electrolyte is relatively slow, resulting in relatively small pore diameter and thick barrier layer. While extrapolating

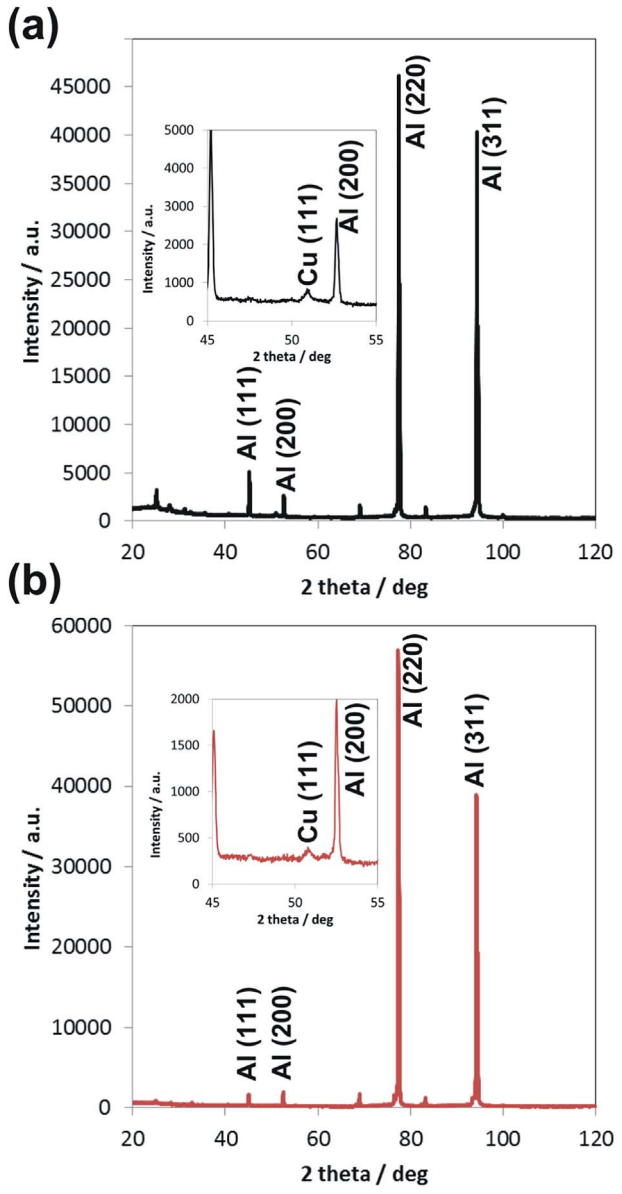

Fig. 6. XRD patterns of Cu nanowires deposited on aluminum substrate with the use of AAO-BLT templates formed at 45 V (a) and 40 V (b).

the empirical relationship reported by Sulka and Parkola [31] for pore diameter increase with voltage, the resulting pore diameter should equal 36 nm. For 30-min long anodizing in 0.3 M oxalic acid at 35 °C, the pore diameter is much greater and equals 49 nm [32], providing a much thinner barrier layer. This results from the fact that the reaction of etching is much more intensive in oxalic acid and at elevated temperature, with simultaneous lower oxide growth rate [31–32].

Recently, it was shown that despite an electrolyte change, when the voltage is maintained, the pores do not tend to interconnect or to form any Y-junctions, what would be undesirable for further applications [33–34]. Nevertheless, in particular cases a kind of fishbone structure is seen at the cross sections of AAO [34]. As one can see in Fig. 2d, the stepwise voltage decrease during the electrochemical barrier layer thinning, BLT, (Fig. 1, reaction IV) resulted in a current response. According to Furneaux et al. [18], Choi et al. [19] and Sauer et al. [20], each step of BLT should be short enough to not re-create a porous structure at lower voltage at the pore bottoms. Thus, the current density vs. time curve cannot achieve a *plateau* of the steady state growth of nanoporous alumina. On the other hand, too short voltage steps in the BLT process will not open the pore bottoms successfully. Therefore, optimization of the electrochemical BLT is required.

As mentioned in the experimental section, four different process conditions of electrochemical barrier layer thinning were investigated in a first attempt to optimize the pore opening procedure. Voltage was reduced stepwise by either 50% (Fig. 3a, e) or 25% (Fig. 3b, f) of its previous value. The duration of each step was fixed at 60 s (Fig. 3a–b) or 10 s (Fig. 3e–f). As it can be seen already from the current density vs. time curve (Fig. 3a), a 50% drop in voltage ($U_{n+1} = 0.5 \cdot U_n$ steps) for $\Delta t = 60$ s is not efficient enough, because no significant current density response was registered. This implied that the oxide barrier layer still provided strong electrical insulation. Fig. 3c (view from the bottom side of the AAO template) shows that at this set of operating conditions, the barrier layer is still present in the form of hemispheres. BLT with shorter, i.e. 10-second long steps, with 50% voltage drop was also found to be unsuccessful (Fig. 3g), despite the different current density response during the consecutive voltage steps (Fig. 3e). On the other hand, when $U_{n+1} = 0.75 \cdot U_n$ steps were applied, distinct current responses were recorded (Fig. 3b, f) and, as a consequence, the barrier layer thinning was found to be successful since complete pore opening was reached (Fig. 3d, h). However, it is noticeable, that the bottoms of the pores in Fig. 3h ($U_{n+1} = 0.75 \cdot U_n$; $\Delta t = 10$ s) are much wider (in fact, almost destroyed after aluminum substrate removal) by the BLT process, whereas the hexagonal honeycomb-like morphology is maintained (Fig. 3d) for longer voltage decrease steps ($U_{n+1} = 0.75 \cdot U_n$; $\Delta t = 60$ s). Thus, numerous but short steps made the pore opening more efficient. It is easy to imagine that at the pore bottoms, wider pores are preferred to guarantee a much better electrical contact with the Al substrate. Thus, for AAO formed at 45 V and opened according to the procedure shown in Fig. 3f and h, the pore diameter at the bottom is approx. 75 ± 13 nm, while at the upper zones (not shown) it is much smaller and equals approx. 42 ± 4 nm.

In order to check the applicability of the AAO formed with combined HA, MA and BLT, electrodeposition of copper was conducted. The novelty of the approach is to form a through-hole oxide template made of ordered alumina nanopores on a conductive aluminum substrate to synthesize Cu nanowires without the need for gold sputtering and electrodeposition prior to it. In Fig. 4, high aspect ratio Cu nanowires are shown formed via electrodeposition into the through-hole AAO template with the evident pore openings (see Fig. 3h). Successful electrodeposition confirmed the efficient barrier layer thinning: sufficient electrical contact at the electrolyte–aluminum interface provided by the BLT process allowed the reduction of Cu^{2+} cations at the pore bottoms. Morphological features of the formed copper nanowires were determined by the morphology of the employed AAO template. The average diameter of the Cu nanowires was 40 ± 5 nm, while their length was 15.7 ± 1.0 μm (Table 1), which corresponds to an aspect ratio of about 400.

In order to expand the applicability of the technique, AAO was also formed at 40 V, and the same BLT approach ($U_{n+1} = 0.75 \cdot U_n$; $\Delta t = 10$ s) was used to obtain the template. It was shown previously that anodization at 40 V also provides well-ordered AAO in both sulfuric acid (HA regime) and oxalic acid (MA regime) [30]. Also in this case, electrodeposition of copper resulted in the formation of nanowires (Fig. 5). The lower voltage of anodization results in the formation of AAO with smaller morphological features. Consequently, copper nanowires with slightly smaller average diameters of 35 ± 6 nm and total lengths of 14.4 ± 2.7 μm (also in this case the aspect ratio was ca. 400) were formed (Table 1). Fig. 6 shows the XRD patterns of Cu nanowires on aluminum substrate formed by electrodeposition into AAO templates formed at 45 V (a) and 40 V (b), respectively. So, the general applicability of through-hole nanoporous AAO templates formed by a combination of hard anodizing and electrochemical barrier layer thinning in the synthesis of Cu nanowires has been confirmed. According to the XRD patterns, the most distinct reflection from copper nanowires

was found for the (111) plane, what is in line with the results reported by Zaraska et al. [13]. However in that case, Cu NWs were grown on a Cu substrate. According to literature data, when copper is deposited in the form on nanowires on a different substrate, the (111) reflection is sometimes the only visible reflection in the XRD pattern [35–36]. It is linked to the penetration depth of X-ray radiation that is tens of microns, while thickness of the nanowires is expressed in tens of nanometers. Nevertheless, a sufficiently high quantity of the nanowires allowed to obtain reflections from the (111) plane.

4. Conclusions

Nanoporous anodic aluminum oxide templates suitable for nanofabrication were formed, employing a multi-step approach, without oxide removal. The novelty of the reported approach is a combination of the high-ordering regime of hard anodizing in sulfuric acid and mild anodizing in oxalic acid with subsequent electrochemical barrier layer thinning. So-formed oxide templates on aluminum substrates allowed for the electrodeposition of copper in the form of high aspect ratio nanowires.

Conducted research allows to draw the following conclusions:

- Cu nanowires were formed by electrodeposition into AAO formed with combined HA-MA-BLT approach.
- It is practically impossible to perform BLT of anodic alumina formed by HA in sulfuric acid. In order to produce AAO with much thinner barrier layers, an electrolyte change to oxalic acid is required.
- The more steps of pore opening during BLT, the more efficient the process. Pore opening was achieved by applying voltage drops of $U_{n+1} = 0.75 \cdot U_n$.
- Efficient electrochemical barrier layer thinning provides good electrical contact at the pore bottoms, thus electrodeposition of metals is possible. The presented method is much easier to perform and less time consuming than the traditional formation of free-standing membranes.

Acknowledgements

W.J. Stepniowski cordially acknowledges financial support from the Polish Ministry of Science and Upper Education (Scholarship for Young, Outstanding Researchers 2015–2018, agreement no. 0432/E-410/STYP/10/2015) and the 3mE-TU Delft Cohesion Project Scheme 2016 (project number: PAS530).

M. Michalska-Domańska cordially acknowledges financial support from the Polish Ministry of Science and Higher Education (Scholarship for Young, Outstanding Researchers 2016–2019, agreement no. 1013/E-410/STYP/11/2016).

References

[1] Ch. Girginov, S. Kozhukharov, M. Milanes, M. Machkova, Impact of the anodizing duration on the surface morphology and performance of A2024-T3 in a model corrosive medium, Mater. Chem. Phys. 198 (2017) 137–144, http://dx.doi.org/10.1016/j.matchemphys.2017.05.049.

[2] H. Masuda, K. Fukuda, Ordered metal nanohole arrays made by a two-step replication of honeycomb structures of anodic alumina, Science 268 (1995) 1466–1468.

[3] M. Mohajeri, H. Akbarpour, Knowledge-based prediction of pore diameter of nanoporous anodic aluminum oxide, J. Electroanal. Chem. 705 (2013) 57–63, http://dx.doi.org/10.1016/j.jelechem.2013.07.026.

[4] Y. Song, L. Jiang, W. Qi, C. Lu, X. Zhu, H. Jia, High-field anodization of aluminum in concentrated acid solutions and at higher temperatures, J. Electroanal. Chem. 673 (2012) 24–31, http://dx.doi.org/10.1016/j.jelechem.2012.03.017.

[5] T. Kikuchi, D. Nakajima, J. Kawashima, S. Natsui, R.O. Suzuki, Fabrication of anodic porous alumina via anodizing in cyclic oxocarbon acids, Appl. Surf. Sci. 313 (2014) 276–285, http://dx.doi.org/10.1016/j.apsusc.2014.05.204.

[6] S. Akiya, T. Kikuchi, S. Natsui, N. Sakaguchi, R.O. Suzuki, Self-ordered porous alumina fabricated via phosphonic acid anodizing, Electrochim. Acta 190 (2016) 471–479, http://dx.doi.org/10.1016/j.electacta.2015.12.162.

[7] Y. Song, H. Wu, B. Yang, J. Wang, J. Yang, C. Xu, X. Zhu, H. Jia, Effect of solvent on the structural features and the degree of ordering of pore arrays in porous anodic alumina, J. Electroanal. Chem. 682 (2012) 110–115, http://dx.doi.org/10.1016/j.jelechem.2012.07.026.

[8] W.J. Stępniowski, M. Norek, B. Budner, M. Michalska-Domańska, A. Nowak-Stępniowska, A. Bombalska, M. Kaliszewski, A. Mostek, S. Thorat, M. Salerno, M. Giersig, Z. Bojar, In-situ electrochemical doping of nanoporous anodic aluminum oxide with indigo carmine organic dye, Thin Solid Films 598 (2016) 60–64, http://dx.doi.org/10.1016/j.tsf.2015.11.084.

[9] M. Salerno, N. Patra, R. Losso, R. Cingolani, Increased growth rate of anodic porous alumina by use of ionic liquid as electrolyte additive, Mater. Lett. 63 (2009) 1826–1829, http://dx.doi.org/10.1016/j.matlet.2009.05.058.

[10] A. Santos, C.S. Law, T. Pereira, D. Losic, Nanoporous hard data: optical encoding of information within nanoporous anodic alumina photonic crystals, Nano 8 (2016) 8091–8100, http://dx.doi.org/10.1039/C6NR01068G.

[11] E. Riccomagno, A. Shayganpour, M. Salerno, Optimization of anodic porous alumina fabricated from commercial aluminum food foils: a statistical approach, Materials 10 (2017) 417–429.

[12] W.J. Stepniowski, W. Florkiewicz, M. Michalska-Domanska, M. Norek, T. Czujko, A comparative study of electrochemical barrier layer thinning for anodic aluminum oxide grown on technical purity aluminium, J. Electroanal. Chem. 741 (2015) 80–86, http://dx.doi.org/10.1016/j.jelechem.2015.01.025.

[13] L. Zaraska, G.D. Sulka, M. Jaskuła, Fabrication of free-standing copper foils covered with highly-ordered copper nanowire arrays, Appl. Surf. Sci. 258 (2012) 7781–7786, http://dx.doi.org/10.1016/j.apsusc.2012.04.148.

[14] J. Kim, W. Yang, Y. Oh, J. Kim, J. Moon, Template-directed fabrication of vertically aligned Cu_2ZnSnS_4 nanorod arrays for photoelectrochemical applications via a non-toxic solution process, J. Alloys Compd. 691 (2017) 457–465, http://dx.doi.org/10.1016/j.jallcom.2016.08.293.

[15] S. Dadras, E. Aawani, Fabrication of YBCO nanowires with anodic aluminum oxide (AAO) template, Phys. B Condens. Matter 475 (2015) 27–31, http://dx.doi.org/10.1016/j.physb.2015.06.016.

[16] A.Y.Y. Ho, L.P. Yeo, Y.C. Lam, I. Rodriguez, Fabrication and analysis of gecko-inspired hierarchical polymer Nanosetae, ACS Nano 5 (2011) 1897–1906, http://dx.doi.org/10.1021/nn103191q.

[17] M. Alsawat, T. Altalhi, T. Kumeria, A. Santos, D. Losic, Carbon nanotube-nanoporous anodic alumina composite membranes with controllable inner diameters and surface chemistry: influence on molecular transport and chemical selectivity, Carbon 93 (2015) 681–692, http://dx.doi.org/10.1016/j.carbon.2015.05.090.

[18] R.C. Furneaux, W.R. Rigby, A.P. Davidson, The formation of controlled-porosity membranes from anodically oxidized aluminium, Nature 337 (1989) 147–149.

[19] J. Choi, G. Sauer, K. Nielsch, R.B. Wehrspohn, U. Gösele, Hexagonally arranged monodisperse silver nanowires with adjustable diameter and high aspect ratio, Chem. Mater. 15 (2003) 776–779, http://dx.doi.org/10.1021/cm0208758.

[20] G. Sauer, G. Brehm, S. Schneider, K. Nielsch, R.B. Wehrspohn, J. Choi, H. Hofmeister, U. Gösele, Highly ordered monocrystalline silver nanowire arrays, J. Appl. Phys. 91 (2002) 3243–3247, http://dx.doi.org/10.1063/1.1435830.

[21] Z. Wu, Y. Zhang, K. Du, A simple and efficient combined AC–DC electrodeposition method for fabrication of highly ordered Au nanowires in AAO template, Appl. Surf. Sci. 265 (2013) 149–156, http://dx.doi.org/10.1016/j.apsusc.2012.10.154.

[22] A.J. Yin, J. Li, W. Jian, A.J. Bennett, J.M. Xu, Fabrication of highly ordered metallic nanowire arrays by electrodeposition, Appl. Phys. Lett. 79 (2001) 1039, http://dx.doi.org/10.1063/1.1389765.

[23] E. Feizi, K. Scott, M. Baxendale, C. Pal, A.K. Ray, W. Wang, Y. Pang, S.N.B. Hodgson, Synthesis and characterisation of nickel nanorods for cold cathode fluorescent lamps, Mater. Chem. Phys. 135 (2012) 832–836, http://dx.doi.org/10.1016/j.matchemphys.2012.05.066.

[24] C.T. Sousa, D.C. Leitao, J. Ventura, P.B. Tavares, J.P. Araújo, A versatile synthesis method of dendrites-free segmented nanowires with a precise size control, Nanoscale Res. Lett. 7 (2012) 168, http://dx.doi.org/10.1186/1556-276X-7-168.

[25] N. Winkler, J. Leuthold, Y. Lei, G. Wilde, Large-scale highly ordered arrays of freestanding magnetic nanowires, J. Mater. Chem. 22 (2012) 16627–16632, http://dx.doi.org/10.1039/c2jm33224h.

[26] M. Norek, M. Dopierała, Z. Bojar, The influence of pre-anodization voltage on pore arrangement in anodic alumina produced by hard anodization, Mater. Lett. 183 (2016) 5–8, http://dx.doi.org/10.1016/j.matlet.2016.07.038.

[27] S.Z. Chu, K. Wada, S. Inoue, M. Isogai, A. Yasumori, Fabrication of ideally ordered nanoporous alumina films and integrated alumina nanotubule arrays by high-field anodization, Adv. Mater. 17 (2005) 2115–2119.

[28] Sachiko Ono, Makiko Saito, Hidetaka Asoh, Self-ordering of anodic porous alumina formed in organic acid electrolytes, Electrochim. Acta 51 (2005) 827–833.

[29] M. Norek, M. Dopierała, W.J. Stępniowski, Ethanol influence on arrangement and geometrical parameters of aluminum concaves prepared in a modified hard anodization for fabrication of highly ordered nanoporous alumina, J. Electroanal. Chem. 750 (2015) 79–88, http://dx.doi.org/10.1016/j.jelechem.2015.05.024.

[30] W.J. Stępniowski, A. Nowak-Stępniowska, A. Presz, T. Czujko, R.A. Varin, The effects of time and temperature on the arrangement of anodic aluminum oxide nanopores, Mater. Charact. 91 (2014) 1–9, http://dx.doi.org/10.1016/j.matchar.2014.01.030.

[31] G.D. Sulka, K.G. Parkola, Anodising potential influence on well-ordered nanostructures formed by anodisation of aluminium in sulphuric acid, Thin Solid Films 515 (2006) 338–345, http://dx.doi.org/10.1016/j.tsf.2005.12.094.

[32] W.J. Stepniowski, Z. Bojar, Synthesis of anodic aluminum oxide (AAO) at relatively high temperatures. Study of the influence of anodization conditions on the alumina structural features, Surf. Coat. Technol. 206 (2011) 265–272, http://dx.doi.org/10.1016/j.surfcoat.2011.07.020.

[33] L. Zaraska, M.M. Jaskuła, G.D. Sulka, Porous anodic alumina layers with modulated pore diameters formed by sequential anodizing in different electrolytes, Mater. Lett.

171 (2016) 315–318, http://dx.doi.org/10.1016/j.matlet.2016.02.113.
[34] L. Zaraska, A. Brudzisz, E. Wierzbicka, G.D. Sulka, The effect of electrolyte change on the morphology and degree of nanopore order of porous alumina formed by two-step anodization, Electrochim. Acta 198 (2016) 259–267, http://dx.doi.org/10.1016/j.electacta.2016.03.050.
[35] H. Kim, S.-H. Choi, M. Kim, J.-U. Park, J. Bae, J. Park, Seed-mediated synthesis of ultra-long copper nanowires and their application as transparent conducting electrodes, Appl. Surf. Sci. 422 (2017) 731–737, http://dx.doi.org/10.1016/j.apsusc.2017.06.051.
[36] H. Yoon, D.S. Shin, B. Babu, T.G. Kim, K.M. Song, J. Park, Control of copper nanowire network properties and application to transparent conducting layer in LED, Mater. Des. 132 (2017) 66–71, http://dx.doi.org/10.1016/j.matdes.2017.06.042.